Oxidation Behavior of Weld Metal, HAZ and Base Metal Regions in Weldments of Cr-Mo Steels

Chromium content was found to significantly affect the oxidation behavior in different regions of the weldment

BY R. K. SINGH RAMAN AND J. B. GNANAMOORTHY

ABSTRACT. In the weldments of 2.25Cr-1Mo and 9Cr-1Mo ferritic steels, the regions with different microstructures were identified as weld metal, heat-affected zone (HAZ) and base metal. When exposed to high temperatures, the HAZ of 2.25Cr-1Mo steel and the weld crown region of 9Cr-1Mo steel were found to oxidize at higher rates, and develop much thicker scale than other regions in the weldments of the respective steels. SEM/EDS point analyses and SIMS depth profiles indicate that the scale over the regions showing inferior oxidation resistance are considerably less in free chromium content. The difference in the oxidation behavior of the different regions was found to arise from the difference in the Cr content of the inner layer of the protective oxide. Possible remedial measures to minimize the high oxidation rates in certain regions of the weldments of the two steels are also discussed.

Introduction

Their adequate creep strength and corrosion resistance make the Cr-Mo ferritic steels a popular choice for steam generating systems in thermal and nuclear power plants (Refs. 1, 2). However, the performance of the welds of these steels is a matter of concern since most of the in-service failures occur in their weldments (Refs. 3–5). Inferior mechanical properties of welds are generally attributed to the undesirable microstructure in certain regions of the weldments (Refs. 4, 6, 7). In recent years, variations in the microstructures of 2.25Cr-1Mo and 9Cr-1Mo steels have also been found to influence their high-temperature corrosion behavior and other associated properties such as cracking/spallation of the oxide scale (Refs. 8–13). These phenomena may also contribute to the failures (Refs. 14–16). For example, while attempting to understand the environmental influence on creep properties, Jackson, *et al.* (Ref. 17), have observed higher corrosion rates and high propensity of failures in the welded structures of 9Cr-1Mo steel. In a similar study on 2.25Cr-1Mo steel weldments, Klueh and King (Ref. 15) have observed faster propagation of cracks along the grain boundaries in the HAZ than those in other regions of the weldments. This could be due possibly to the formation of Cr-rich secondary phases and corresponding depletion of free Cr along the grain boundaries, which could result in an increase in oxidation in such areas that could also assist crack propagation. The observations of Klueh and King (Ref. 15) and those of Jackson, *et al.* (Ref. 17), though, deal mainly with the mechanical properties of the weldments of 2.25Cr-1Mo and 9Cr-1Mo steels. They certainly entail detailed investigations on the oxidation behavior of the microstructurally different regions in the weldments of the two popular alloys. Such investigations may help in understanding the contribution, if any, of corrosion to the inferior in-service performance of the welds of the steels.

The present study relates to the high-temperature corrosion of the weldments of 2.25Cr-1Mo and 9Cr-1Mo steels, showing difference in the oxidation behavior in microstructurally varying regions. The weldments used for this study had not experienced any postweld heat treatment (PWHT) that is normally given to the weldments. Therefore, these investigations may be considered as a maiden attempt to understand the high-temperature corrosion behavior of the as-welded Cr-Mo steels, which will be followed by further investigations to compare the present results with the corrosion behavior of the postweld heat-treated weldments. If temperature-time schedules for the PWHT's for the two steels are not carefully chosen, it can cause precipitation of Cr-rich carbides in the HAZ, as well as the weld metal, resulting in further deterioration in the corrosion resistance of these regions.

KEY WORDS

Oxidation Behavior
Weld Metal
Heat-Affected Zone
Base Metal
Cr-Mo Ferritic Steel
High-Temp. Effects
Corrosion
Oxidation Rate
Oxide Scale
Oxidation Resistance

Experimental Procedure

Normalized-and-tempered (N and T) plates, 12 mm thick (0.36 in.), of 2.25Cr-1Mo steel were welded together by shielded metal arc welding (SMAW) using basic covered electrodes of composition similar to the plates. Similarly, the N and T plates of 9Cr-1Mo steel were also welded by the SMAW process using

R. K. SINGH RAMAN is presently with School of Materials Science and Engineering, University of New South Whales, Sydney, Australia, and J. B. GNANAMOORTHY are with Metallurgy Division, Indira Gandhi Center for Atomic Research, Kalpakkam, India.

Table 1 — Chemical Compositions (wt-%)

Steel	Region in Weldment	C	Si	S	P	Cr	Mo
2.25 Cr-1Mo steel	Base metal	0.06	0.18	0.008	0.008	2.18	0.93
	Weld metal	0.05	0.40	0.020	0.012	2.30	1.10
9Cr-1 Mo steel	Base metal	0.10	0.497	0.004	0.03	8.4	0.96
	Weld metal	0.12	0.520	0.003	0.03	8.9	0.98

Table 2 — Welding Conditions for 2.25 Cr-1 Mo and 9Cr-1 Mo Steels

Process	Shielded metal arc
Preheat	473 K
Arc current	110—120 A
Electrode diameter	3.15 mm
Arc voltage	22 V
Number of passes	8–10
Welding speed	3.75 mm/s

a basic covered electrode of similar composition. The chemical compositions of the base metal and the deposited weld metal of the two steels are given in Table 1. The welding conditions for the two steels are detailed in Table 2.

Using a diamond-coated wafering saw, and by careful metallography, specimens of weld metal, HAZ and base metal were cut out of the weldments of 2.25Cr-1Mo steel — Fig. 1A. Since the scaling behavior of the root (lower) region of the weld metal was found to he different from that of the crown (upper) part of the weld (to be discussed later), specimens of both upper and lower parts of the welds, as well as those of the HAZ and the base metal, were separated out of the weldments of 9Cr-1Mo steel — Fig. 1B. The HAZ being a narrow region, it was ascertained by repeated cycles of polishing, etching and microscopic examinations that the HAZ specimens used for oxidation tests consisted only of the microstructure of the HAZ, and there were no contributions from the adjoining regions, *i.e.*, the weld metal and the base metal regions. Out of the remaining portions of the weld pads of the two steels, 2-mm-thick (0.08-in.) transverse sections consisting of all the three different regions of the weldments were sliced — Fig. 2. The specimens of weld metal, HAZ and base metal (Fig. 1), and those of the transverse sections of the weldment (Fig. 2), were mechanically ground, polished up to 1 μm diamond finish, cleaned with a detergent, and washed in acetone. The polished and cleaned specimens were oxidized in a muffle furnace in air. Oxidation tests were carried out for a maximum of 500 h, at 773 K (932°F) for 2.25Cr-1Mo steel, and at 923 K for 9Cr-1Mo steel. Weight gains of the specimens of weld metal, HAZ and base metal were measured after different lengths of time up to 500 h. During these interruptions, the difference in thickness of the oxide scales developed over the regions with different microstructure in the weldments of the two steels were measured using a surface profilometer. Morphological features of the surfaces and cross-sections of the oxide scales developed over the different regions of the weldments of the two steels were observed using scanning electron microscopy (SEM), and the chemical characterization of the scales was done by energy dispersive analyses of x-rays (EDS) and secondary ion mass spectrometry (SIMS). Surface profilometric technique has been used to investigate the change in the surface profiles of the oxide scales formed over the microstructurally different, neighboring regions in the weldments of 2.25Cr-1Mo and 9Cr-1Mo steels. For this purpose, a Sloan DEKTAK 3030 surface profile measuring system was employed, which can accurately measure vertical features ranging in height from 50 angstroms to 131 μm. Measurements are made electromechanically by moving the sample beneath a diamond-tipped stylus coupled to a linear variable differential transformer (LVDT). For the present measurements, a diamond tipped stylus with an impressed force of 0.1 mN was made to ride over the surfaces of the oxidized specimens. There was a vertical deflection whenever the stylus encountered an unevenness in topography, such as those due to difference in thicknesses of the oxide scales over the heat-affected zone and the weld metal of the steels.

Experimental details of oxidation tests and postoxidation analyses can be found elsewhere (Ref. 14).

Experimental Results

Oxidation Behavior of Different Regions of Weldments of 2.25Cr-1Mo Steel

All of the three regions of the weld-

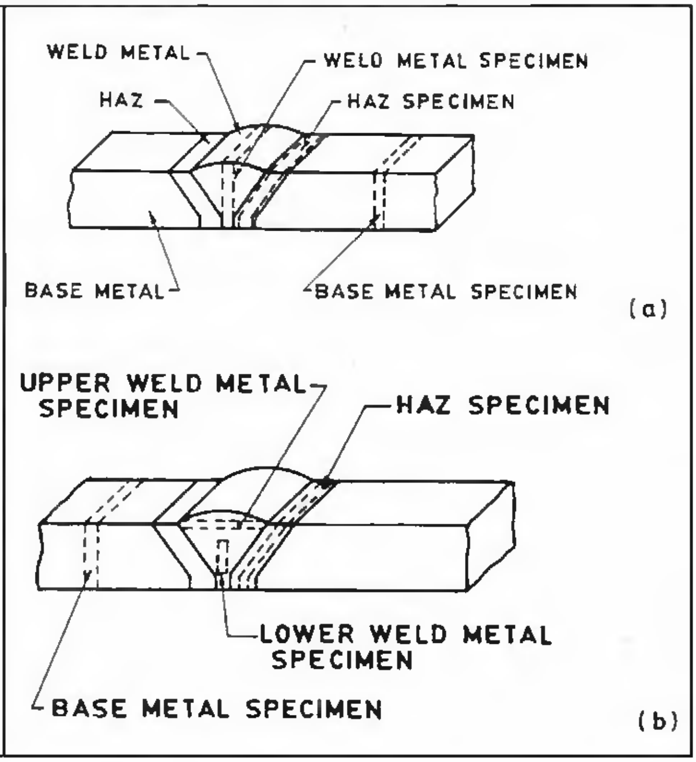

Fig. 1 — Schematic diagram showing the locations of different regions in the weldments and the cuts for separating samples of these regions. A — weldments of 2.25Cr-1Mo steel; B — weldments of 9Cr-1Mo steel.

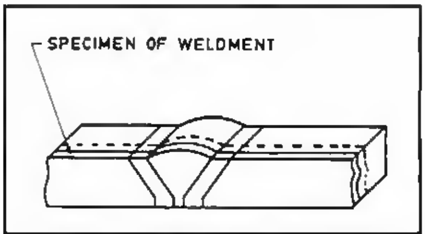

Fig. 2 — Schematic diagram showing sections of weldment (consisting of weld metal, HAZ and base metal) cut out of a weld pad.

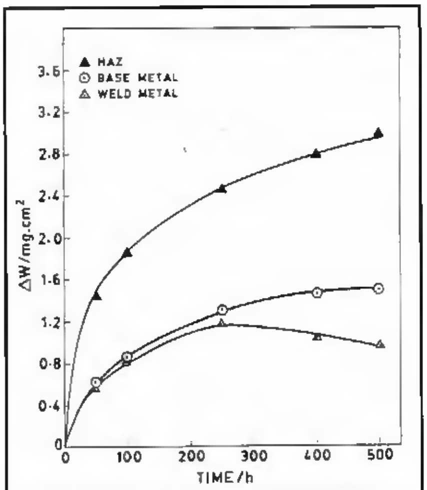

Fig. 3 — Weight gain vs. time plots for weld metal, HAZ and base metal separated out of the weldments of 2.25Cr-1Mo steel, and oxidized in air at 773 K for 500 h.

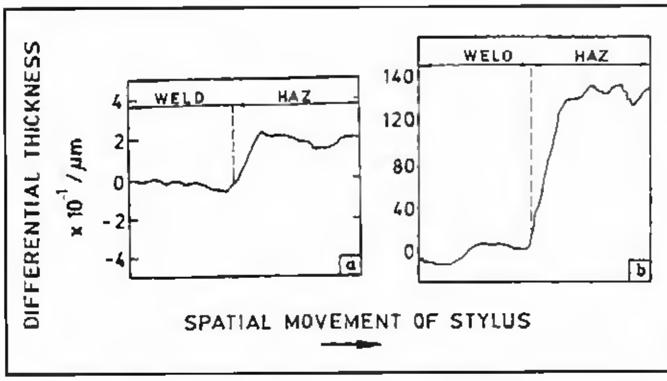

Fig. 4 — Surface profiles describing the difference in thicknesses of oxide scale over weld metal of 2.25Cr-1Mo steel, oxidized in air at 773 K. A — 2 h; B — 500 h.

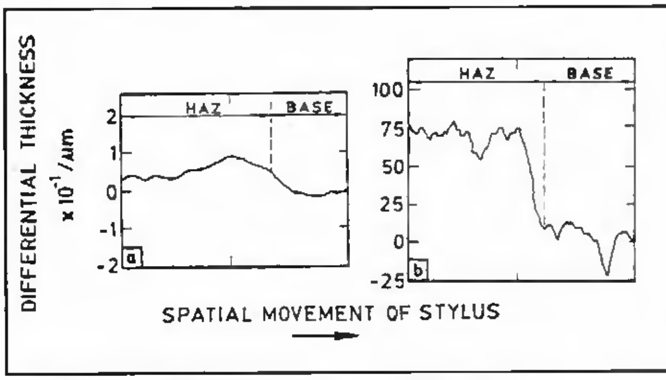

Fig. 5 — Surface profiles describing the difference in thicknesses of oxide scale over HAZ and base metal of 2.25Cr-1Mo steel, oxidized in air at 773 K. A — 2 h; B — 500 h.

ment, *i.e.*, the weld metal, the heat-affected zone (HAZ) and the base metal followed parabolic kinetics during their oxidation at 773K for 500 h — Fig. 3. However, the HAZ region oxidized at a much higher rate than the weld metal and the base metal, both of which oxidized at similar rates. As a result, at the end of a 500 h-test, the weight gained by the HAZ was more than twice the weight gained by the weld metal/base metal. A higher oxidation rate of the HAZ could also be corroborated by results of the surface profilometry (Figs. 4, 5), which suggested a considerable greater thickness of oxide scale developed over the HAZ compared to that over the weld metal and the base metal regions. Optical and SEM micrographs (Figs. 6, 7) also suggest the formation of scale of greater thickness and larger grain size over the HAZ than over other regions. Greater thickness of the scale over the HAZ could be further corroborated by the SEM micrographs of the cross-sections of the oxidized specimens of the weldments — Fig. 8. These micrographs suggest that after 100 h oxidation thickness of the scale formed over the HAZ was around 9 μm greater than those of the scale formed over the weld metal and the base metal.

Chromium content of the inner layer of oxide (*i.e.*, the layer near the inner boundary of the oxide scale), as characterized from the EDS analyses of the cross-sections of the scale (Fig. 8), provided a significant clue for the difference in oxidation rate of the different regions. Scale over the HAZ had considerably less Cr in the inner layer than at the similar location of the scale over the weld metal and the base metal — Fig. 8. The trend of higher Cr content in the weld metal scale is confirmed by the depth profiles of Fe, Cr and O in the scale (developed in 4 h), over the weld metal, the HAZ and the base metal — Fig. 9. The profiles of the three regions unambiguously indicate higher peak heights for Cr in the inner scale over the weld metal and the base metal than that in the HAZ scale. The relative contents of Fe and Cr (Fe/Cr ratios at such depths) in the innermost scales, *i.e.*, at a depth where Cr is highest, show considerably higher Cr contents in the inner oxide scale of the weld metal (Fe/Cr: 2.03) and the base metal (Fe/Cr : 2.31) than that in the inner scale formed over the HAZ (Fe/Cr: 4.12). Interestingly, the difference in thicknesses of the oxide scale over the weld metal and the HAZ (about 1.4 μm), as seen from the depth profiles of oxygen for the two scales, does not corroborate with the results of the surface profiles, which had indicated a difference of about 1.0 μm after 4 h of oxidation. This ambiguity suggests a greater possibility of internal oxidation in the HAZ.

Oxidation Behavior of Different Regions of Weldments of 9Cr-1Mo Steel

The four regions of the weldment, namely the upper and lower welds, the HAZ and the base metal (Fig. 1B) oxidized at different rates when exposed for 500 h in air at 923 K (1202°F). However, unlike in the case of 2.25Cr-1Mo steel

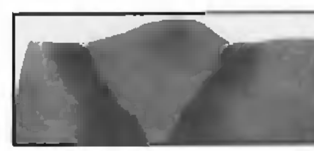

Fig. 6 — Optical photographs describing the difference in the appearance of the oxide scale over weld metal, HAZ and base metal of 2.25Cr-1Mo steel, oxidized at 773 K for 4 h.

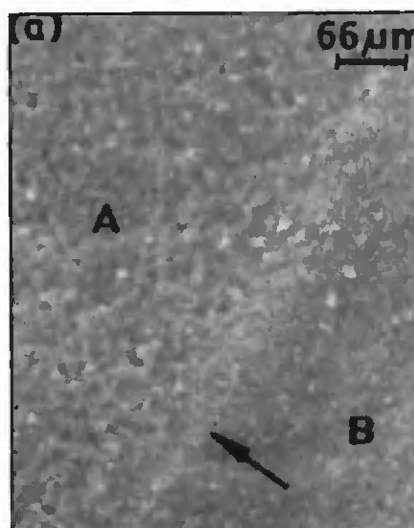

Fig. 7 — Scanning electron micrographs comparing oxide scale formed over: A — HAZ and B — weld metal of 2.25 Cr-1Mo steel oxidized at 773 K for 100 h. Arrowhead indicates the interface between the two regions.

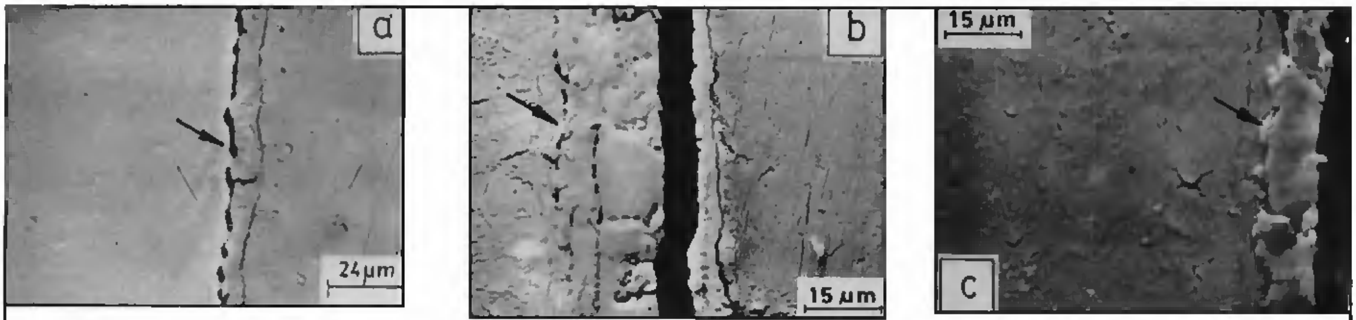

Fig. 8 — Scanning electron micrographs showing the cross-sections of the oxide scale formed over A — weld metal, B — HAZ and C — base metal of the weldments of 2.25Cr-1Mo steel oxidized at 773 K for 100 h. Fe/Cr ratios near the inner boundary of the oxide (scale indicated by arrowheads): A — 7.6 in weld metal inner oxide, B — 17.2 in HAZ inner oxide, and C — 6.9 in base metal oxide.

(Fig. 3), it was the weld metal that oxidized at much higher rates than the other regions — Fig. 10. The oxidation rate decreased in the order: the upper surface of the weld metal (*i.e.*, the weld crown), the lower surface of the weld metal, the HAZ and the base metal. There was a marked difference in the thicknesses of the scales formed over the weld metal and the HAZ (0.45 µm in 4 h, and 18.5 µm in 500 h of oxidation, Fig. 11). The SEM photomicrograph in Fig. 12 indicates a sharp difference in the morphologies, owing to the coarse- and fine-grained scale, respectively, over the upper weld metal and the HAZ. The oxide scale grown over the lower weld metal was less coarse as compared to that over the upper weld metal — Fig. 13; the boundary between the scale over the two regions was somewhat diffuse. As indicated in Fig. 12, Cr content of the oxide scale over the base metal, the HAZ and the lower weld metal, as analyzed by EDS, was significantly higher than that of the oxide scale formed over the upper weld metal. A comparison of the SIMS depth profiles of Fe, Cr and O in the scale over the different regions (Figs. 14, 15) also suggests a greater thickness of the oxide scale formed over the upper and lower weld metal regions than the scale over the HAZ and the base metal regions. More importantly, a comparison of these profiles indicates considerably lower peak heights of Cr in the inner layer of the scale over both the weld metal regions than those in the base metal and the HAZ scale, though the thickness of the Cr-containing inner layer was greater in the scale developed on the weld metal.

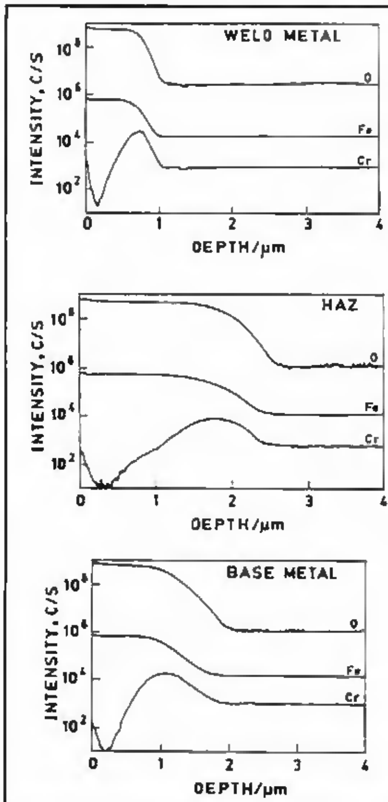

Fig. 9 — SIMS depth profiles of Fe, Cr and O in the oxide scale formed over different regions of weldment: A — weld metal (in the inner scale where Cr peaks, Fe/Cr: 2.03), B — HAZ (in the inner scale, Fe/Cr: 4.12), and C — base metal (in the inner scale, Fe/Cr: 2.31). The depth profiles were taken using Cs+ primary bombardment and collecting negative secondary ions.

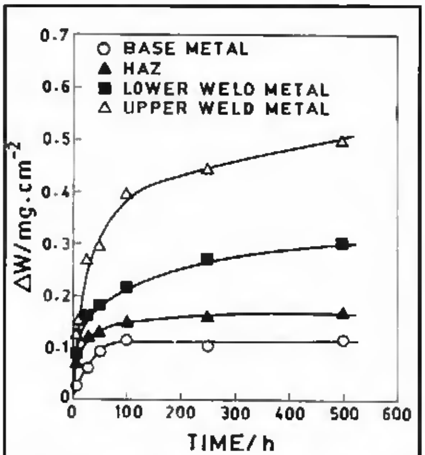

Fig. 10 — Weight gain vs. time plots for base metal, HAZ, and the upper (crown) and lower (root) regions separated out of the weldments of 9Cr-1Mo steel, and oxidized in air at 923 K for 500 h.

Discussion

Oxidation resistance of the Fe-Cr alloys, including the Cr-Mo ferritic steels, is influenced by the chromium content of the inner layer of protective Fe-Cr oxide (Refs. 8–10, 12). Thus, the higher oxidation rate leading to formation of thicker oxide scales over the HAZ of the 2.25Cr-1Mo steel (Fig. 4) and over the weld metal of 9Cr-1Mo steel (Fig. 11) can be attributed to the lower Cr content of the inner scale formed over this region, as suggested by the respective results of the SIMS and EDS analyses — Figs. 8, 9, 12, 14, 15. Lower Cr content renders the scale less protective by facilitating the diffusion of iron and oxygen involved in the oxidation reaction. This allows oxidation to occur at higher rates and formation of thicker outer scale, as observed in the case of the HAZ of 2.25Cr-1Mo steel, and the weld metal region of 9Cr-1Mo steel. Thus, the results of the oxidation tests and the post-oxidation analyses of the different regions of the weldments of the two steels appear to be well in agreement. However, one needs to find an answer to why should there be a variation in Cr contents in the inner layer of the oxides over the microstructurally different regions of the weldment of the same steel. Here, it would be mandatory to recall that depletion of free Cr from the alloy matrix through the precipitation of Cr-rich phases can result in an inner scale with less Cr content, and this in turn can influence the oxidation resistance of Cr-Mo ferritic steels (Refs. 8–10, 12, 14, 17, 18). Hence, what remains to be addressed is the physiochemical aspects of depletion of free Cr through secondary precipitation in the regions of the weldments of the two steels showing different oxidation rates.

The secondary precipitates in the HAZ of 2.25Cr- 1 Mo steel, as reported by Roy and Lauritzen (Ref. 19), would be M_7C_3, $M_{23}C_6$ and M_6C, while Mo_2C would be virtually absent in the HAZ. On the other hand, the secondary precipitates reported to form in normalized and tempered 2.25 Cr-1Mo steel base metal (Ref. 20-22), would be Fe_3C and Mo_2C. Lundin, *et al.* (Ref. 4), have identified Fe_3C and Mo_2C as the only carbides that occur in the microstructure of the weld metal. Recently, TEM investigations by Singh Raman, *et al.* (Refs. 8, 23), have also confirmed the insignificant population of needle-shaped precipitates (Mo_2C), and occurrence of parallelpiped and rod-shaped precipitates (M_7C_3, $M_{23}C_6$ and M_6C) in the HAZ, as well as the occurrence of Mo_2C exclusively in the weld metal and the base metal regions of the weldments of 2.25Cr-1 Mo steel (without PWHT). Hence, Cr present in the weld metal and the base metal regions of the weldment of this steel is relatively free and available for formation of complex Fe-Cr oxides (that is protective) in the inner scale. Klueh and King (Ref. 15) have made a similar observation, while describing the environmental influences on the creep rupture behavior of the dissimilar welds of 2.25Cr-1Mo steel. They have also reported the formation of Fe_3O_4 in the grain boundary notches/cracks in the HAZ region (where the failures are mostly found to occur), and have attributed the formation of this Fe-rich oxide to the Cr depletion along the grain boundaries in the HAZ by carbide precipitation.

There is a dearth of information on the types and degree of precipitation in the different regions of the weldments of 9Cr-1Mo steel. The precipitation behavior of this steel austenitized at different temperatures has been investigated in detail by Pickering and Vassiliou (Ref. 24), and has been described through the isothermal transformation diagrams. These diagrams can be very useful in understanding the free Cr contents of the different regions of the weldment. It is important to note that Cr-rich carbide, $M_{23}C_6$ (mostly, as $Fe_5Cr_{18}C_6$) and Cr_2N are the only secondary phases reported to form in 9Cr-1Mo steel (Refs. 24, 25). A certain amount of delta-ferrite may also be present in the weld metal (Refs. 26, 27). The presence of delta-ferrite in the microstructure can decrease the free Cr content of this steel, owing to the facts that the presence of delta-ferrite is known to cause early precipitation of secondary phases even during rapid cooling (Refs. 24, 25), and also because the retained delta-ferrite in the high-Cr steels is a Cr-rich phase. Hence, the observed lower Cr content of the inner scale, and the higher oxidation rate, in general, of the weld metal (for both crown and root regions of the weld metal) can be attributed to the delta-ferrite formation resulting in the increased propensity for precipitation of Cr-based secondary phases. Jackson, *et al.* (Ref. 17), have also indicated the higher corrosion rate of the weld metal of 9Cr-1Mo steel, and they have attributed this behavior to the precipitation of Cr-based carbides in the weld metal. However, the lower part of the weld metal shows a lower oxidation rate than the upper region. It is understood that the root (lower) region of the weld metal that was formed from the initial passes was subjected to reheating during the subsequent passes (in the multipass welding employed for the present study). This reheating might have aided the redissolution of $M_{23}C6$ and Cr_2N precipitates resulting in increased free Cr. However, the very quick rise in temperature and the subsequent fast cooling might have allowed neither the complete redissolution nor the reprecipitation of the secondary phases in this region. In the absence of delta-ferrite and little precipitation of Cr-based secondary phases in the HAZ and the base metal regions, it is possible that most of the chromium in these regions was available for formation of the protective scale, and hence the oxidation resistance of these regions was superior to the upper and lower regions of the weld metal.

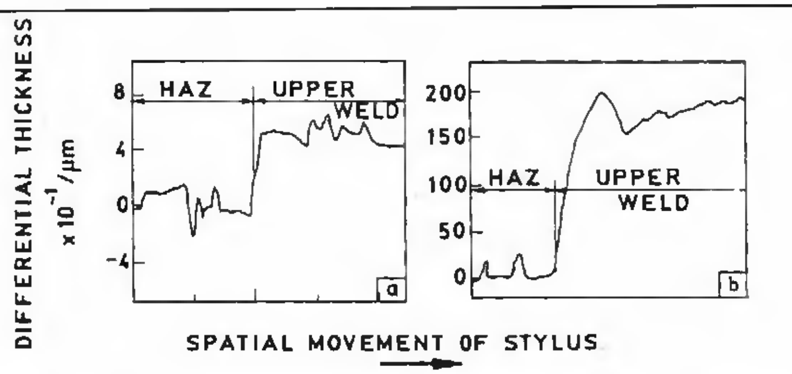

Fig. 11 — Surface profiles describing the difference in thicknesses of oxide scale over the upper region of the weld metal and the HAZ of 9Cr-1Mo steel, oxidized at 923 K for: A — 4 h; B — 500 h.

Conclusions

1) When oxidized at 773 K in air, the heat-affected zone (HAZ) of the weldment of 2.25Cr-1Mo steel oxidizes at a

Fig. 12 — Scanning electron micrographs comparing morphologies of oxide scale formed over upper portion (A) of the weld metal and HAZ (B) in the weldment of 9Cr-1Mo steel oxidized at 923K for: A — 100 h; B, C — 500 h.

Fig. 13 — Scanning electron micrographs comparing oxide scales formed over the upper (A) and lower (B) regions of weld metal of 9Cr-1Mo steel oxidized for 100 h.

much higher rate and develops a thicker oxide scale than the base metal and the weld metal.

2) The higher oxidation rate of the HAZ of 2.25Cr- 1Mo steel and the formation of a thicker scale over it have been attributed to the less protective inner oxide scale, due possibly to the nonavailability of free Cr from the alloy as a result of carbide formation in this region.

3) When weldment of 9Cr-1Mo steel is oxidized at 923 K in air, the upper region of the weld metal oxidizes at a higher rate, and develops a thicker oxide scale than the other regions of the weldment. Thickness of the scales formed over different regions decreases in the order: the upper portion of the weld metal, the lower weld metal, the HAZ, the base metal.

4) The higher oxidation rate and the thicker oxide scale formation over the crown (upper) weld region of 9Cr-1Mo steel could be attributed to the least protective inner scale of Fe-Cr oxides with minimum Cr content.

Acknowledgments

The authors are thankful to A. K. Tyagi for his interest and active involvement in SIMS analyses, and to K. Laha for his help in preparation of the weldments and in understanding the physical metallurgy of the weldments of the two steels. The authors are also grateful to T. P. S. Gill for useful discussions. Thanks are also due to M. Radhika for her help in SEM/EDX analyses.

References

1. *Proc. BNES Int. Conf. Ferritic Steels for Fast Reactor Steam Generators*, 1978. eds., S. F. Pugh and E. A. Little, London, England.

2. *Application of 2.25Cr-1Mo Steel for Thick-Walled Pressure Vessel*. 1982. ASTM STP 755, American Society for Testing and Materials, Philadelphia, Pa.

3. *ASME Boiler and Pressure Vessel Code*. 1986. Code Case N-47.

4. Lundin, C. D., Kelly, S. C., Menon, R., and Kruse, B. J. 1984. Stress rupture behavior of postweld heat treated 2.25Cr-1Mo steel weld metal, Welding Research Council Bulletin No. 315, pp. 1–66.

5. Chew, B., and Harris, P. 1979. *Metal Construction*, 11: 11.

6. Laha, K., Bhanu Sankara Rao, K., and Mannan, S. L. 1990. *Mater. Sci. Eng.*, A129, p. 183.

7. Arnswald, W., Blum, R., Neubaur, B., and Poulson, K. E. 1986. *Proc. Int. Conf. Creep*, Tokyo, Japan, pp. 367–372.

8. Singh Raman, R. K., Ph.D. Thesis. 1993. Influence of variations in alloy microstructure on high temp. corrosion of 2.25Cr-1Mo and 9Cr-1Mo steels, IIT, Kharagpur, India.

9. Singh Raman, R. K., Khanna, A. S., and Gnanamoorthy, J. B . 1990. Proc. 1st. Int. Conf. on Microscopy of Oxidation, eds., M. J. Bennett and G. W. Lorimer, Cambridge, England, pp. 54–64.

10. Singh Raman, R. K., and Gnanamoorthy, J. B. 1992. J. Mater. Sci., 27: 3435.

11. Singh Raman, R. K., Khanna, A. S., Tiwari, R. K., and Gnanamoorthy, J. B. 1992. *Oxid. Met.*, 37: 1.

12. Singh Raman, R. K., Khanna, A. S., Choudhary, B. K., and Gnanamoorthy, J. B. 1991. *Mater. Sci. Eng.*, A148, p. 299.

13. Singh Raman, R. K., and Gnanamoorthy, J. B., *Oxid. Met.*, 38 (1992)483

14. Singh Raman, R. K., and Gnanamoorthy, J. B. 1993. *Corr. Sci.*, 34: 1275.

15. Klueh, R. L., and King, J. F. 1982. *Welding Journal* 61: 302-s.

16. Hancock, P. 1977. *Vacancies 76*. eds., R. E. Smallman and J. E. Harris, The Metal Soc., London, England, p. 215.

17. Jackson, P. W., Chadwick, M. D., and Graham B. L. 1978. *Proc. BNES Conf on Ferritic Steels for Fast Reactor Steam Generators*. eds., S. F. Pugh and E. A. Little, London, England, p. 488.

18. Singh Raman, R. K., Gnanamoorthy, J. B., and Roy, S. K. 1994. *Oxid. Met.*, 40: 21.

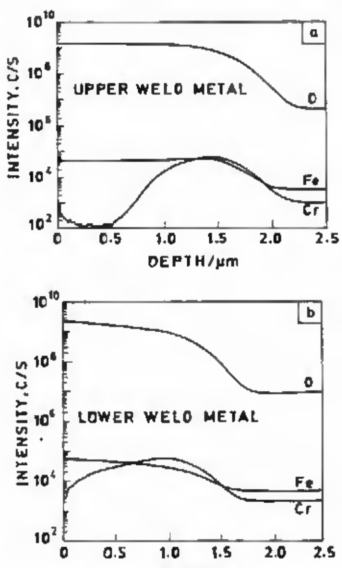

Fig. 14 — SIMS depth profiles of Fe, Cr and O in the oxide scales formed at 923 K in 1 h, over different regions of weldment of 9Cr-1 Mo steel: A — upper portion of weld metal (in the inner scale where Cr peaks, Fe/Cr : 1.04), B — lower portion of weld (in the inner scale, Fe/Cr : 0.65). The depth profiles were taken using Cs+ primary bombardment and collecting negative secondary ions.

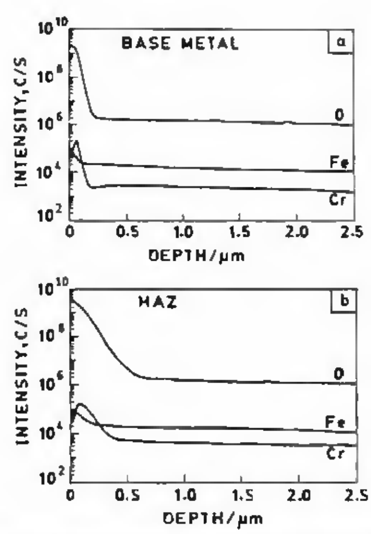

Fig. 15 — SIMS depth profiles of Fe, Cr and O in the oxide scales formed at 923 K in 1 h, over different regions of weldment of 9Cr-1Mo steel: A — base metal (in the inner scale where Cr peaks, Fe/Cr : 0.23), and B — HAZ (in the inner scale, Fe/Cr : 0.26). The depth profiles were taken using Cs+ primary bombardment and collecting negative secondary ions.

19. Roy, P., and Lauritzen, T. 1984. *Welding Journal* 6: 455.
20. Baker, R. G., and Nutting, J. 1959. *J. Iron Steel Inst.* 192: 275.
21. Hippsley, C. A. 1981. *Met. Sci.*, 10: 137.
22. Pilling, J. and Ridley, N. 1982. *Metall. Trans. A.* 13A: 557.
23. Singh Raman, R. K., and Iyagi, A. K. 1994. *Mater. Sci. Eng.*, A185: 97.
24. Pickering, F. B. and Vassiliou, A. D. 1980. *Met. Technology*, p. 408.
25. Sanderson, S. J. 1978. *Proc. BNES Conf.*, p. 120.
26. Fidler, R. S., and Gooch, D. J., *ibid.*, p. 128.
27. Edmonds, D. P., and Chew, B., CEGB Report, TPRD/M/1258/N82.

ELEVATED TEMPERATURE TESTING OF GASKETS FOR BOLTED FLANGED CONNECTIONS

by M. Derenne, L. Marchand, J. R. Payne, and A. Bazergui

Gasket performance data and technical formulations which would permit the design of gasket systems for high-temperature service were studied to better understand flange behavior, gasket deformation, and leakage behavior under simulated elevated-temperature service conditions. This WRC Bulletin discusses the results obtained for the four areas covered in the study:

♦ The extrapolated long-term elevated-temperature performance of compressed asbestos-reinforced sheet materials.

♦ The effect of the creep/relaxation of flexible graphite sheet marerials at elevated temperatures on the tightness of a joint in which the gasket deflection remains practically constant.

♦ The effect of the gas medium and pressure on the tightness performance at elevated temperature of graphite-filled spiral-wound gaskets with and without internal rings.

♦ The correlations between the weight loss of elastomeric sheet gasket materials during aging at elevated temperatures and the changes in their mechanical properties and tightness performance — leading to the proposal of a new aging parameter, based on weight loss correlation and successfully grouping the data obtained for different test times and temperatures.

Publication of this document was sponsored by the Pressure Vessel Research Council.

The price of WRC Bulletin 391 (May 1994) is $60 per copy plus $5 postage and handling for U.S. and Canada, and $10 for overseas. Orders should be sent with payment to Welding Research Council, 345 E. 47th St., Room 1301, New York, NY 10017; (212) 705-7956; FAX (212) 371-9622.